

Glaucoma Imaging

Antonio Ferreras
Editor

 Springer

Glaucoma Imaging

Antonio Ferreras
Editor

Glaucoma Imaging

 Springer

Editor
Antonio Ferreras
Ophthalmology
Miguel Servet University Hospital
Zaragona
Spain

ISBN 978-3-319-18958-1 ISBN 978-3-319-18959-8 (eBook)
DOI 10.1007/978-3-319-18959-8

Library of Congress Control Number: 2015950942

Springer Cham Heidelberg New York Dordrecht London
© Springer International Publishing Switzerland 2016

This work is subject to copyright. All rights are reserved by the Publisher, whether the whole or part of the material is concerned, specifically the rights of translation, reprinting, reuse of illustrations, recitation, broadcasting, reproduction on microfilms or in any other physical way, and transmission or information storage and retrieval, electronic adaptation, computer software, or by similar or dissimilar methodology now known or hereafter developed.

The use of general descriptive names, registered names, trademarks, service marks, etc. in this publication does not imply, even in the absence of a specific statement, that such names are exempt from the relevant protective laws and regulations and therefore free for general use.

The publisher, the authors and the editors are safe to assume that the advice and information in this book are believed to be true and accurate at the date of publication. Neither the publisher nor the authors or the editors give a warranty, express or implied, with respect to the material contained herein or for any errors or omissions that may have been made.

Printed on acid-free paper

Springer International Publishing AG Switzerland is part of Springer Science+Business Media
(www.springer.com)

Contents

1	Standard Automated Perimetry	1
	Francisco Javier Goñi and Krapez Maja	
2	Gonioscopy	27
	Michele Figus, Maurizio Taloni, and Chiara Posarelli	
3	Measurement of Intraocular Pressure with Goldmann Applanation Tonometry, Dynamic-Contour Tonometry, and Ocular Response Analyzer	79
	Paolo Fogagnolo, Maurizio Digiuni, and Luca Rossetti	
4	Ultrasound Biomicroscopy in Glaucoma	97
	Julián García-Feijoo, Carmen Méndez-Hernández, José María Martínez de la Casa, Federico Sáenz-Francés, Rubén Sánchez-Jean, and Julián García-Sánchez	
5	Retrobulbar Ocular Blood Flow Evaluation in Open-Angle Glaucoma	123
	Antonio Martinez	
6	Optic Nerve Head Assessment and Retinal Nerve Fiber Layer Evaluation	149
	Antonio Ferreras	
7	Confocal Scanning Laser Ophthalmoscopy	173
	Michele Iester	
8	Detection of Glaucoma Using Scanning Laser Polarimetry	209
	Patricio G. Schlottmann and Pilar Calvo	
9	Optical Coherence Tomography	227
	Paolo Frezzotti	

10	Measuring Hemoglobin Levels in the Optic Nerve Head for Glaucoma Management	265
	Manuel Gonzalez-de-la-Rosa, Marta Gonzalez-Hernandez, Carmen Mendez-Hernandez, Elena Garcia-Martin, Francisco Fumero-Bautista, Silvia Alayon, and Jose Sigut	
11	Structure and Function Relationship in Glaucoma	281
	Rizwan Malik and David F. Garway-Heath	
12	Assessment of Structural Glaucoma Progression	305
	Francesco Oddone	

Chapter 10

Measuring Hemoglobin Levels in the Optic Nerve Head for Glaucoma Management

**Manuel Gonzalez-de-la-Rosa, Marta Gonzalez-Hernandez,
Carmen Mendez-Hernandez, Elena Garcia-Martin,
Francisco Fumero-Bautista, Silvia Alayon, and Jose Sigut**

10.1 Introduction

The color of the optic nerve head (ONH) is mainly due to its hemoglobin content. The ganglion cell axons may not have myelin at this level. Like the rest of the retina, this tissue is virtually transparent to radiation of the visible spectrum. In the rest of the retina, light is eventually absorbed by photoreceptors and the pigmentary epithelium, but in the ONH the light is reflected by the myelin in the lamina cribrosa. Part of it is absorbed by hemoglobin in the capillaries that nourish the axons, giving rise to the pink color of the ONH. The greater the thickness of the tissue or its concentration of hemoglobin, the more intense the color, and the thinner the tissue or the less abundance of blood, the whiter it will appear (Fig. 10.1).

In a color photograph of the ONH, the results also depend on additional factors such as the chromatic response of the camera's detector, the spectral composition of the illumination light and absorption by the lens, which is more pronounced in blue and increases with age or the presence of cataracts.

To determine the amount of hemoglobin present in the ONH, using a photographic color image, all these factors must be taken into account. Fortunately, we have a structure in the nerve itself that can serve as a reference; this structure is the network of

M. Gonzalez-de-la-Rosa (✉) • M. Gonzalez-Hernandez
Department of Ophthalmology, Hospital Universitario de Canarias,
University of La Laguna, La Laguna, Spain
e-mail: mgdelarosa@telefonica.net

C. Mendez-Hernandez
Department of Ophthalmology, Hospital Clinico San Carlos,
University Complutense of Madrid, Madrid, Spain

E. Garcia-Martin
Department of Ophthalmology, Hospital Universitario Miguel Servet, Zaragoza, Spain

F. Fumero-Bautista • S. Alayon • J. Sigut
Department of Systems Engineering, University of La Laguna, La Laguna, Spain

central retinal vessels carrying hemoglobin. On comparing the color of neuronal tissue and that of these vessels, one can estimate the amount of hemoglobin in each region of tissue with little influence of the additional factors listed in the previous paragraph.

Hemoglobin absorbs more green radiation than red. It can be shown experimentally that for a relatively thin structure such as the ONH, the ratio of green component to red ($(R-G)/R$) is proportional to its thickness or its hematic content. Measuring this ratio in each zone of the tissue and taking the same measurement in the main vessels as a reference, one can obtain a representative map of local amounts of hemoglobin. This is very probably the most important factor for ONH perfusion. Other parameters to consider include the degree of oxygenation and the rate of blood circulation (Fig. 10.2).

The Laguna ONhE program (Optic Nerve Hemoglobin; insoftsl@gmail.com ©) allows measuring the amounts of hemoglobin present in the structures of the ONH, analyzing photographs captured by a fundus camera that has been appropriately calibrated. The program has demonstrated its capacity for the diagnosis and interpretation of glaucomatous damage, as well as other types of neurological damage such as that seen in multiple sclerosis or Parkinson's disease.

In the text that follows, we will describe the use of the program and provide some examples of practical results.

Fig. 10.1 The pink color of the optic nerve head depends on the hemoglobin contained in its capillaries. The observation light is reflected on the myelin, and that not absorbed by hemoglobin, mainly red, reaches the observer

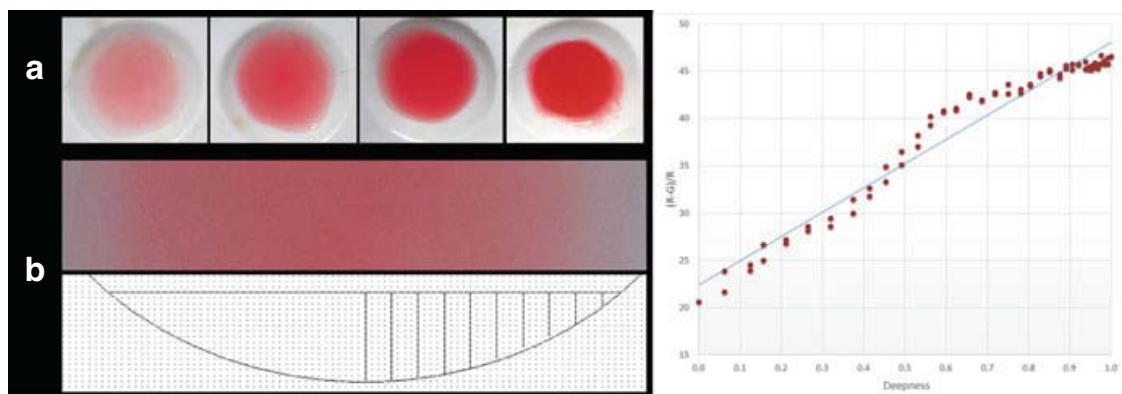
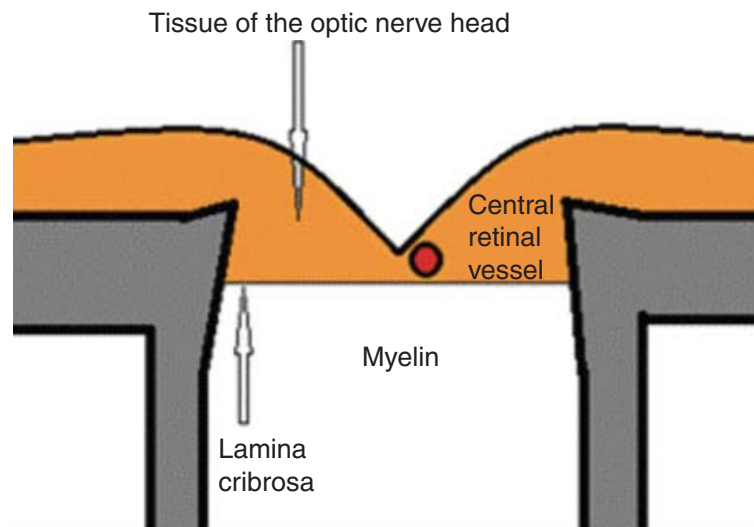


Fig. 10.2 If one photographs microplate wells containing dilutions of hemoglobin (a), the red and green components of the image will be proportional to the concentration and depth (b) of the layer through which the light passes, as shown in the graph on the right

10.2 Image Capture of the ONH and Delimitation of Boundaries, Vessels, and Cup

When a fundus image is captured with the intention of examining the retina, the ONH image often appears too white, without details. This is because it is a much paler structure than the rest of the fundus. For useful results and visualization of ONH details, it is necessary to underexpose the photograph, using a flash of lower intensity than usual. In a very bright image, the color levels of the camera detector reach their maximum value (255) and this saturation prevents seeing the chromatic characteristics of the tissue.

Initial versions of the Laguna ONhE program required manual definition of the ONH boundaries. Delimitation of the cup was not possible and, therefore, the ONH was divided into 24 regular sections by two circular lines at 1/3 and 2/3 of the radius, and four regularly spaced diameters. Analysis of all these sectors allowed us to calculate a glaucoma discriminant function (GDF) that has been shown to be useful for detecting the presence of perfusion defects characteristic of glaucoma, particularly affecting sectors 8 and 20. It even allows us to estimate the vertical cup/disc ratio without defining their precise form (Fig. 10.3).

A second version of the program allowed us to transpose the cup and disc boundaries obtained with OCT to a photographic image of the ONH, so that we could separately determine the amount of hemoglobin in the cup and in the various sectors of the neuroretinal rim (Fig. 10.4). Another version exploited the delimitation of these structures performed with a stereoscopic fundus camera to obtain similar information.

More recently these advances have allowed us to establish a relationship between the distribution of hemoglobin and the size and shape of the cup, so it has been possible to define its boundaries with great precision, without the need for OCT information or stereoscopic photography, simply using a conventional photograph.

Applying methods of image segmentation based on color patterns and identification of the components compatible with the shape of the ONH, it has been possible to automatically establish the boundaries of the ONH in 90 % of cases, without operator intervention. With the image of the ONH on the screen, a click of the mouse on the center of the ONH cues the program to automatically suggest the boundaries of the cup and disc, which must be accepted by the user (Fig. 10.5).

Incorrect delimitation of the boundaries with this automatic method is rare, but can occur especially in cases with areas of atrophy close to the ONH or other unusual morphology. In these cases the user can rectify the disc boundaries at their discretion. To do so an ellipse is projected on the ONH. The center of the ellipse and its shape can be changed using the mouse, until it fits the boundaries. When this configuration is confirmed, multiple points appear on radial axes, which can be adjusted one by one to fit the exact shape of the ONH (Fig. 10.6).

Once the ONH boundaries have been established, estimation of the cup is performed automatically in all cases, since automatic delimitation is generally more accurate than anything the user can achieve on a two-dimensional image. Similarly, internally, the program performs an automatic delimitation of the central retinal artery and vein and its main branches, excluding tissue information, and for use as a reference value of hemoglobin.

Fig. 10.3 Example of segmentation of the ONH in 24 sectors

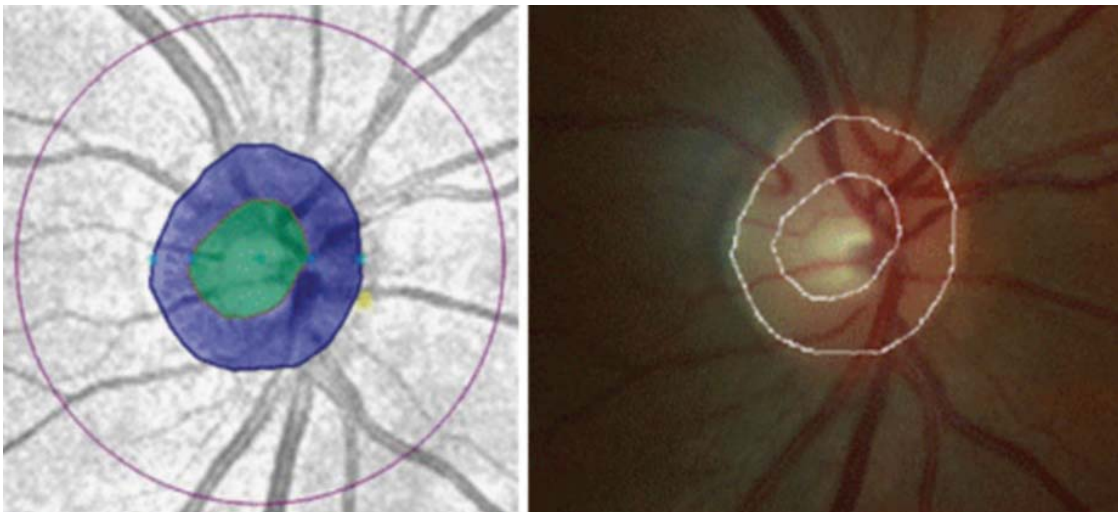


Fig. 10.4 Fusion of an OCT image (*left*) and a photograph of the ONH (*right*) to delimit the boundaries of the cup and disc

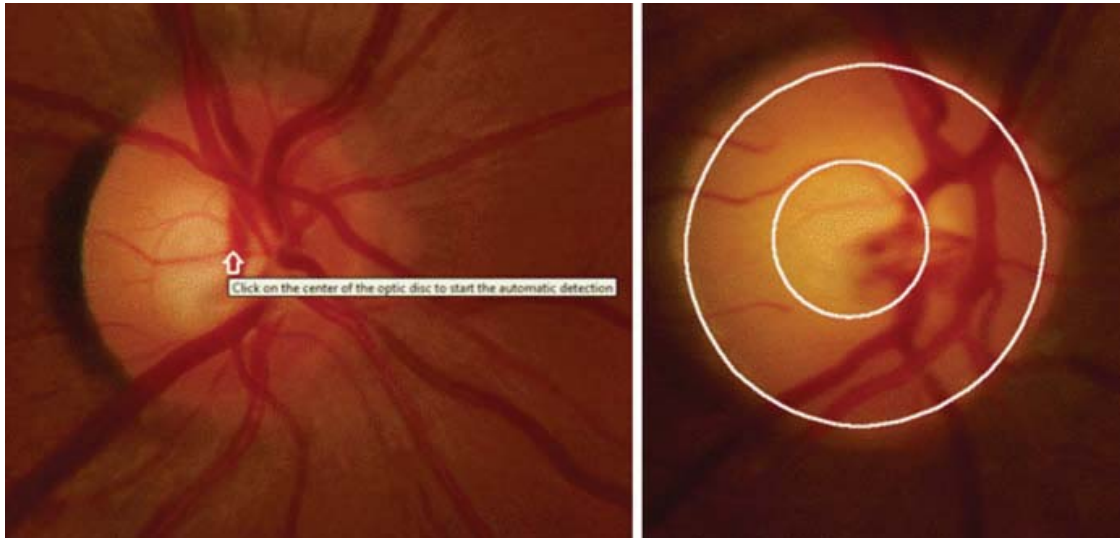


Fig. 10.5 By clicking on the center of the image (*left*), one obtains the cup and disc boundaries (*right*) which must be accepted

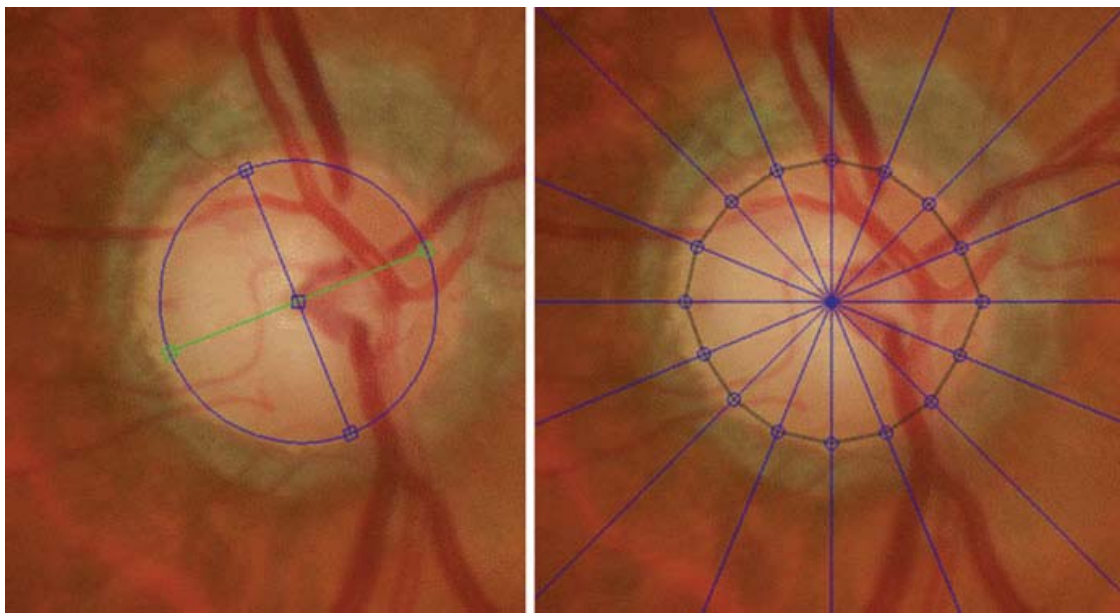


Fig. 10.6 Approximate delimitation using an ellipse (*left*) and fine-tuning using multiple radial points (*right*)

10.3 Hemoglobin Map

After boundary delimitation, the program automatically interprets whether the image is of a right or left eye, asking for user confirmation. It then shows the representative map of the presence of hemoglobin in each region of the ONH. A chromatic scale identifies these amounts of hemoglobin in percentages; 100 % corresponds to the central vessels of the retina. Warmer colors represent high densities of hemoglobin and cooler colors represent areas of lower perfusion or thin tissue, as in the case of cup (Figs. 10.7 and 10.8).

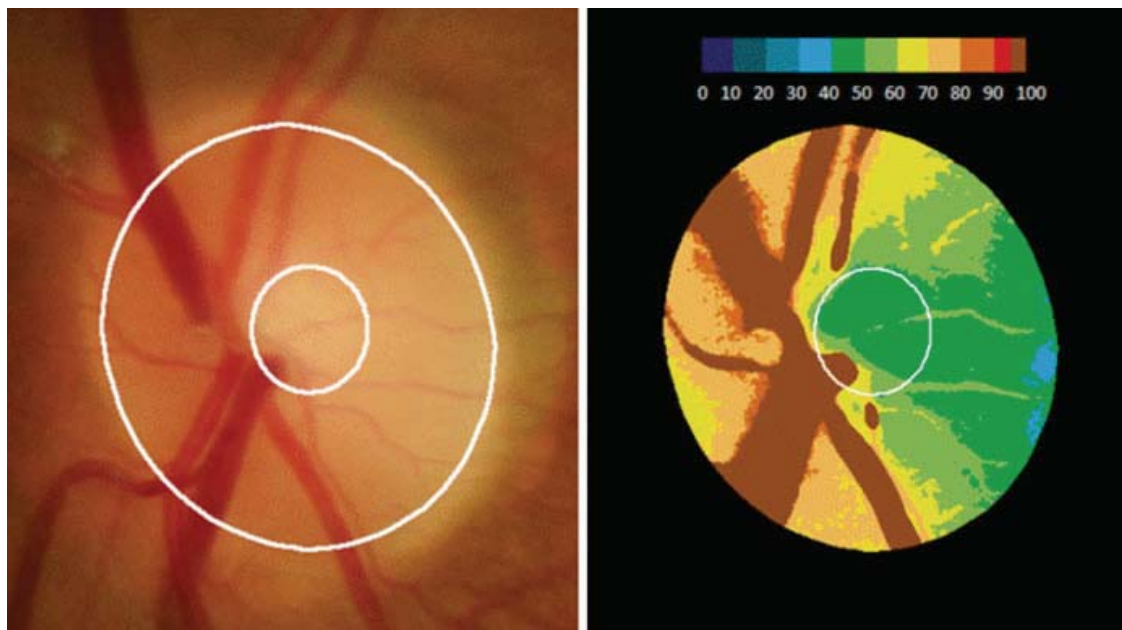


Fig. 10.7 Example of a hemoglobin map in a normal subject, with disc and cup delimitation

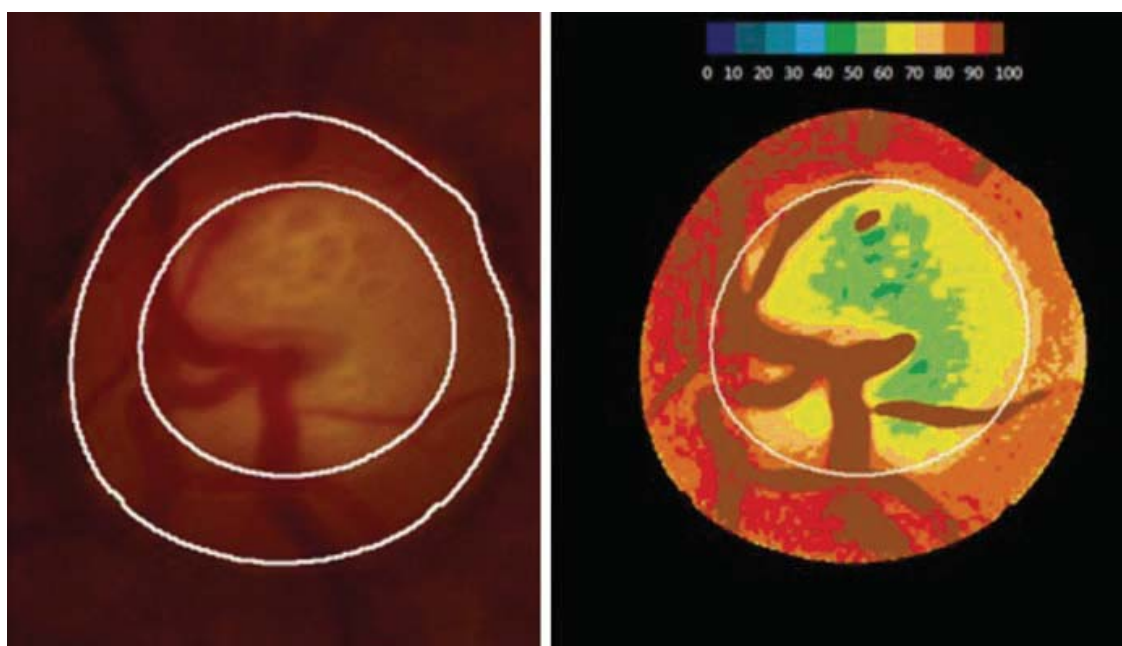


Fig. 10.8 Example of a hemoglobin map in glaucoma

10.4 Glaucoma Discriminant Function (GDF)

In glaucoma, it is well known that there is often greater deterioration of the ONH in areas close to the superior and inferior pole regions. Indeed, using the Laguna ONhE program, lower perfusion is usually found in the vicinity of its central vertical diameter, especially in the extreme and intermediate zones (e.g., sectors 8 and 20), as the subject loses tissue in the neuroretinal rim. Other regions, such as the temporal rim region (Sector 15), are more resistant to glaucomatous damage, which in effect show less impairment of perfusion.

The topographic distributions of hemoglobin allow us to estimate the vertical ratio cup/disc ratio as well as an index called “glaucoma discriminant function” (GDF) which has been shown to have high diagnostic capacity. This index tends to be positive in normal subjects and negative in glaucomatous subjects, which is useful for monitoring the disease. It has been adjusted for a specificity close to 95 %, so that negative values are infrequent in normal subjects, and highly negative values very infrequent (Figs. 10.9, 10.10 and 10.11).

Although the program attempts to compensate for the presence of cataracts, this circumstance may occasionally cause slight overestimation of hemoglobin. Moderate opacification of the lens has a negligible effect. Only with cataracts that require surgical intervention does this overestimation reach approximately 3–4 %. However, estimated cup/disc ratio and GDF index are not affected by the presence of this type of cataract (Fig. 10.12).

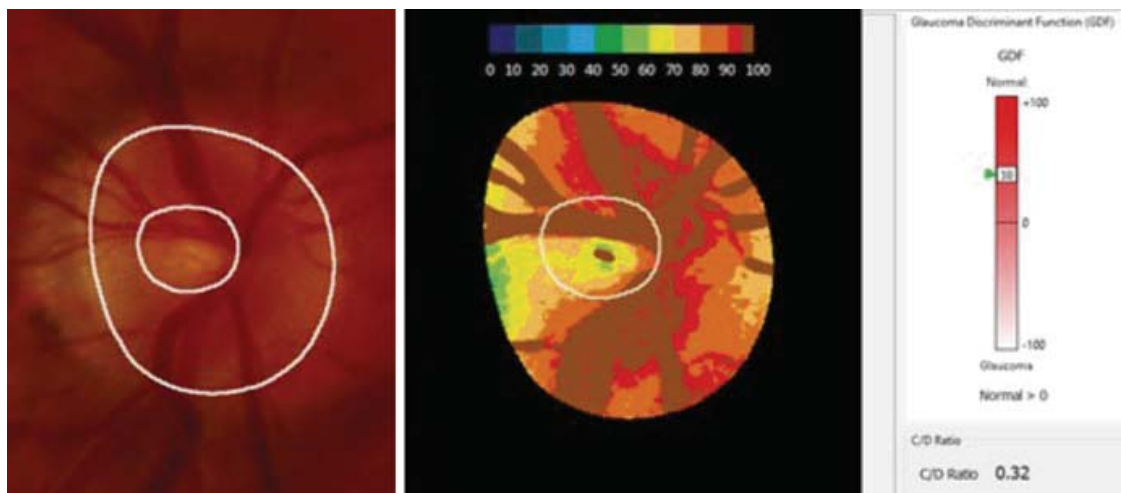


Fig. 10.9 Hemoglobin map and GDF in a normal case

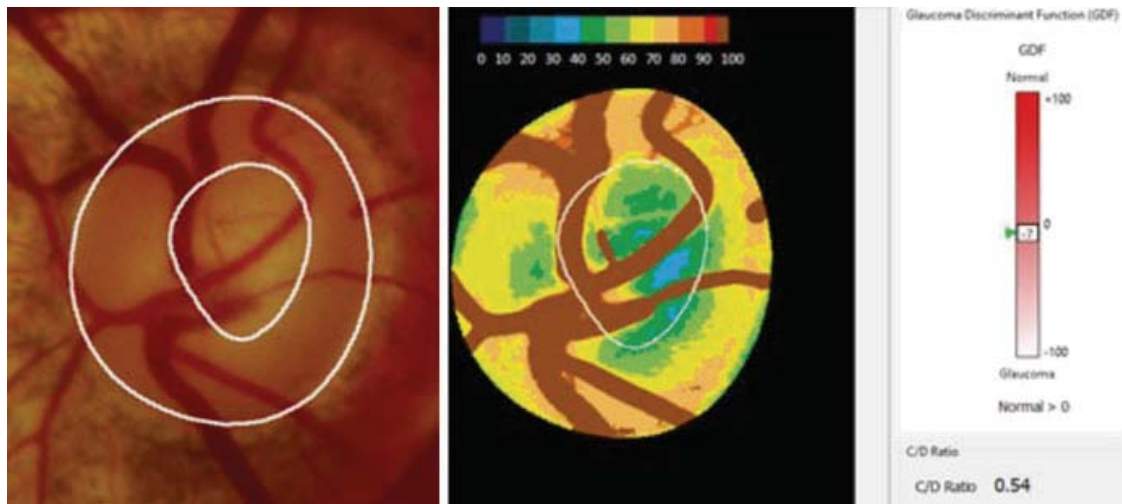


Fig. 10.10 Hemoglobin map and GDF in early glaucoma

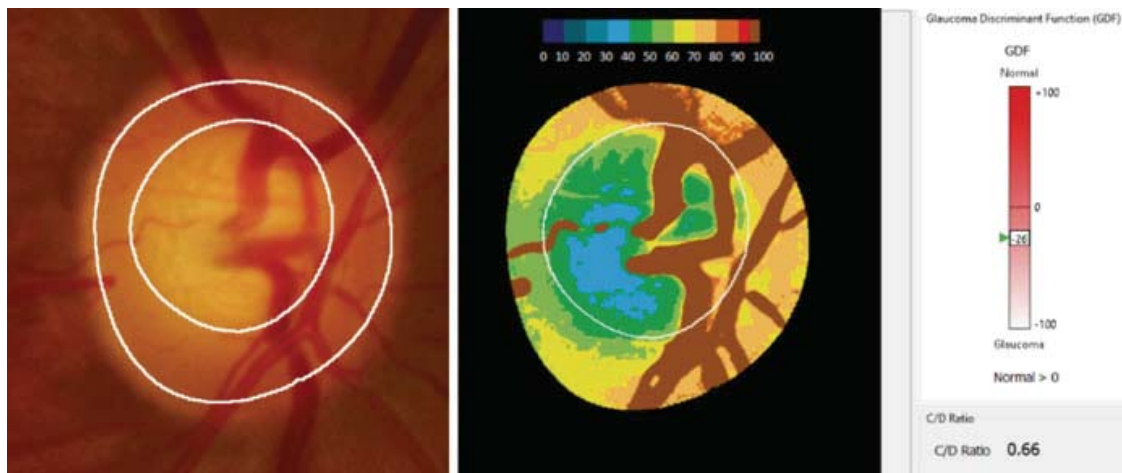


Fig. 10.11 Hemoglobin map and GDF in advanced glaucoma

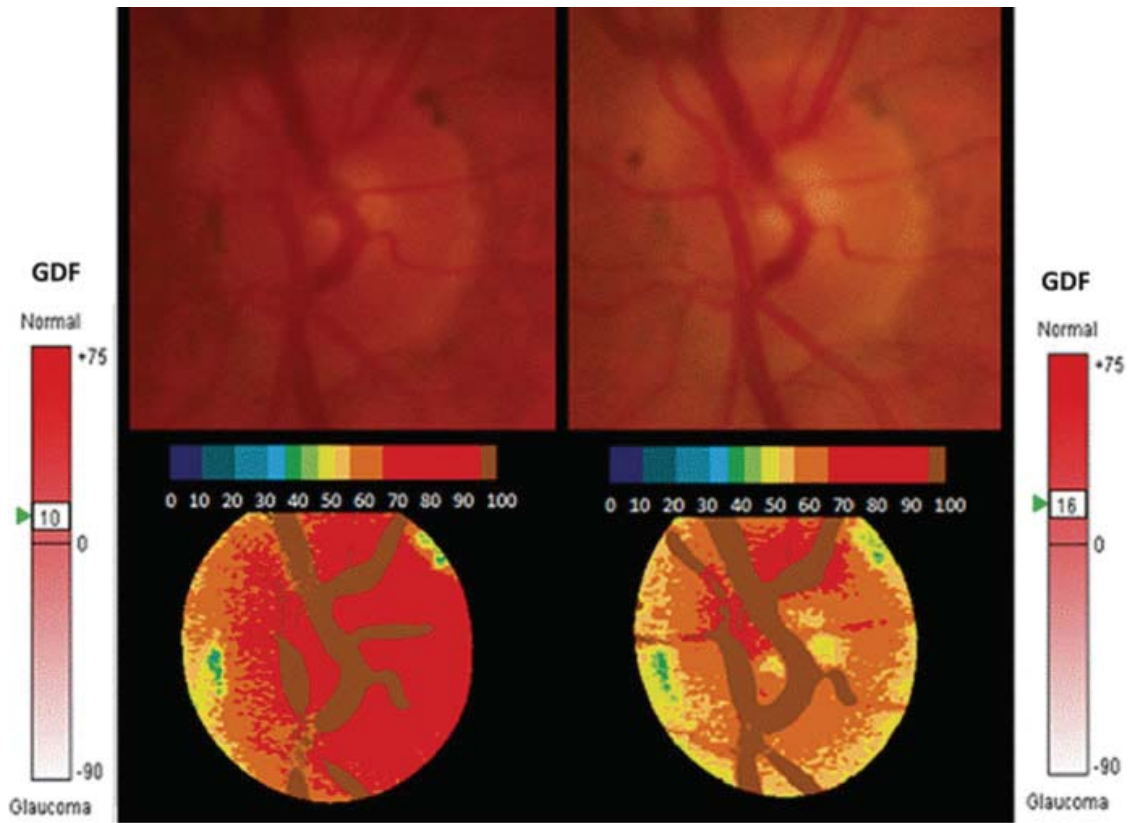


Fig. 10.12 Hemoglobin map and GDF before and after cataract operation in a patient with a normal optic nerve

10.5 Rim Hemoglobin

The program also provides information on the amount of hemoglobin present in the eight sectors into which the rim is usually divided, compared to the normal population. It has been shown that these perfusion data are better correlated with the patient's visual field sensitivity than mere measurement of the rim area, which can be obtained using OCT, for example. It has also been shown that rim surface area in many glaucoma patients is not only lost, but that hemoglobin content in the residual rim is often lower than normal (Fig. 10.13).

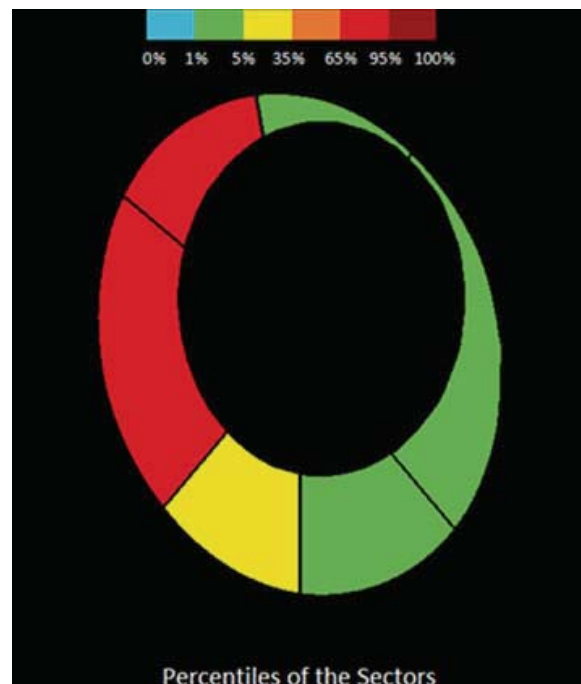


Fig. 10.13 Figure showing the percentile of rim hemoglobin data in the patient mentioned in Fig. 10.11, with respect to the normal population

10.6 TSNI Diagram

Another way to view the results is a diagram similar to that usually used to represent the thickness of the nerve fiber layer around the ONH. In this case the amount of hemoglobin present in the neuroretinal rim is represented starting with the temporal region and followed by the superior, nasal, and inferior regions (TSNI). The diagram simultaneously shows color-coded percentiles of these densities in the normal population, so they can be compared with those of the subject (Fig. 10.14).

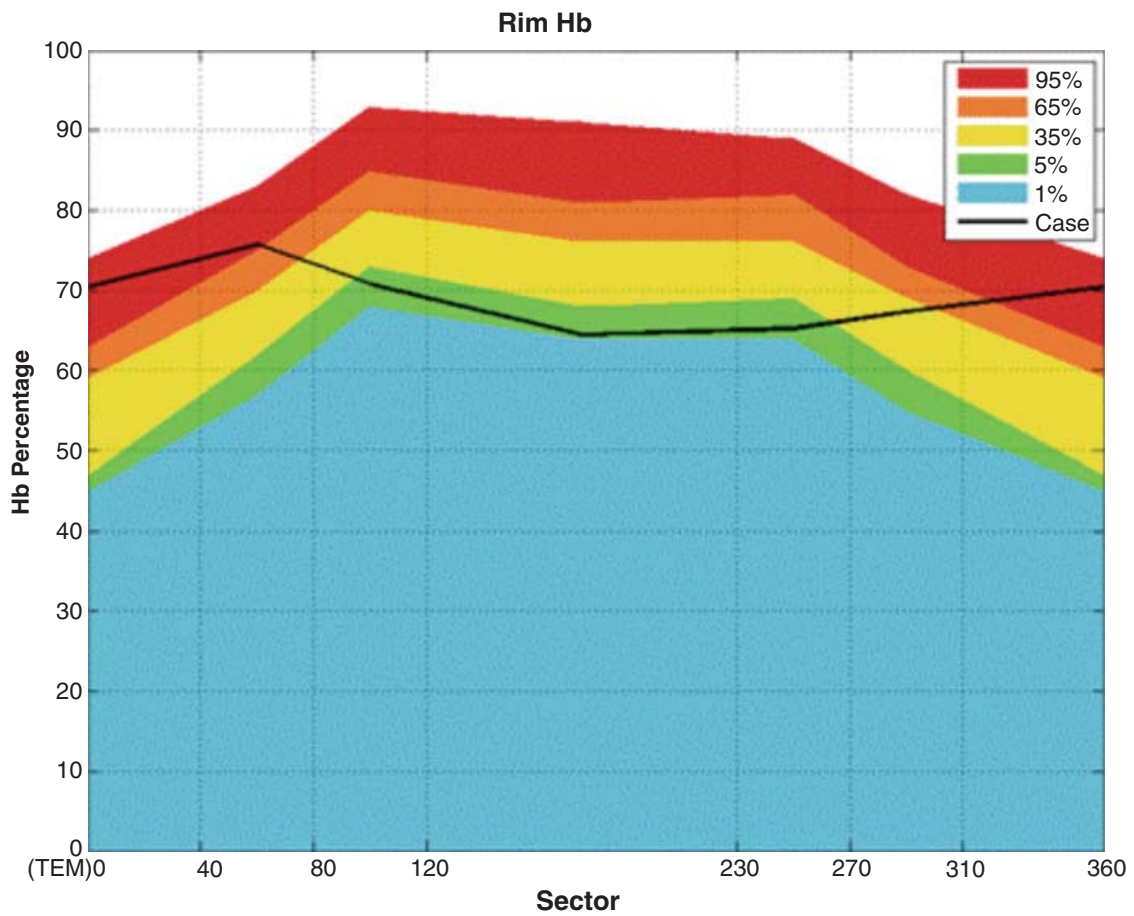


Fig. 10.14 TSNI diagram showing the amounts of hemoglobin in the rim of the same glaucoma subject mentioned in Figs. 10.11 and 10.13

10.7 Sector Hemoglobin: Numerical Data

To calculate the GDF index and the vertical cup/disc ratio, the program divides the ONH into 24 sectors as previously described. The amounts of hemoglobin in each of these sectors, as well as those in the 8 sectors of the rim, are displayed in the form of a table, which also shows their percentile relative to that of the normal population (Fig. 10.15).

This information may be useful in other diseases such as optic neuritis where reduced perfusion may be found in different regions from those affected in glaucoma. In multiple sclerosis, for example, reduced perfusion is most frequently observed in area 15 or the temporal rim, which is not usually the case in glaucoma (Fig. 10.16).

	Mean Hb	Percentiles of the Hb					
		0 - 1%	1 - 5%	5 - 35%	35 - 65%	65 - 95%	95 - 100%
Total	60.9			60.9			
Cup Hb	54.0			54.0			
Sector 311-40° (T)	70.4					70.4	
Sector 41-80°	75.8					75.8	
Sector 81-120°	70.9		70.9				
Sector 121-230°	64.4		64.4				
Sector 231-270°	65.2		65.2				
Sector 271-310°	67.3			67.3			
Sector 1	65.8			65.8			
Sector 2	55.6	55.6					
Sector 3 (N)	65.6			65.6			
Sector 4	68.1			68.1			
Sector 5	50.1	50.1					
Sector 6 (NI)	69.0			69.0			
Sector 7	68.0				68.0		
Sector 8	61.1			61.1			
Sector 9 (I)	75.0			75.0			
Sector 10	55.7				55.7		
Sector 11	64.4					64.4	
Sector 12 (TI)	71.4					71.4	
Sector 13	54.6				54.6		
Sector 14	64.0					64.0	
Sector 15 (T)	73.5						73.5
Sector 16	53.1			53.1			
Sector 17	62.0				62.0		
Sector 18 (TS)	78.7					78.7	
Sector 19	43.8			43.8			
Sector 20	49.5	49.5					
Sector 21 (S)	66.3	66.3					
Sector 22	48.9			48.9			
Sector 23	44.0	44.0					
Sector 24 (NS)	56.6	56.6					

Fig. 10.15 Table showing numerical results of the previous case



Fig. 10.16 Temporal perfusion defect in a case of optic neuritis due to multiple sclerosis

10.8 Data Export and Analysis

The total and sectorial index results and the diagnostic results of each test can be exported to an Excel file and printed out. This also facilitates statistical analysis of the results. The Excel spreadsheet includes graphic representations of patient data, which can be used in workshops and presentations (Fig. 10.17).

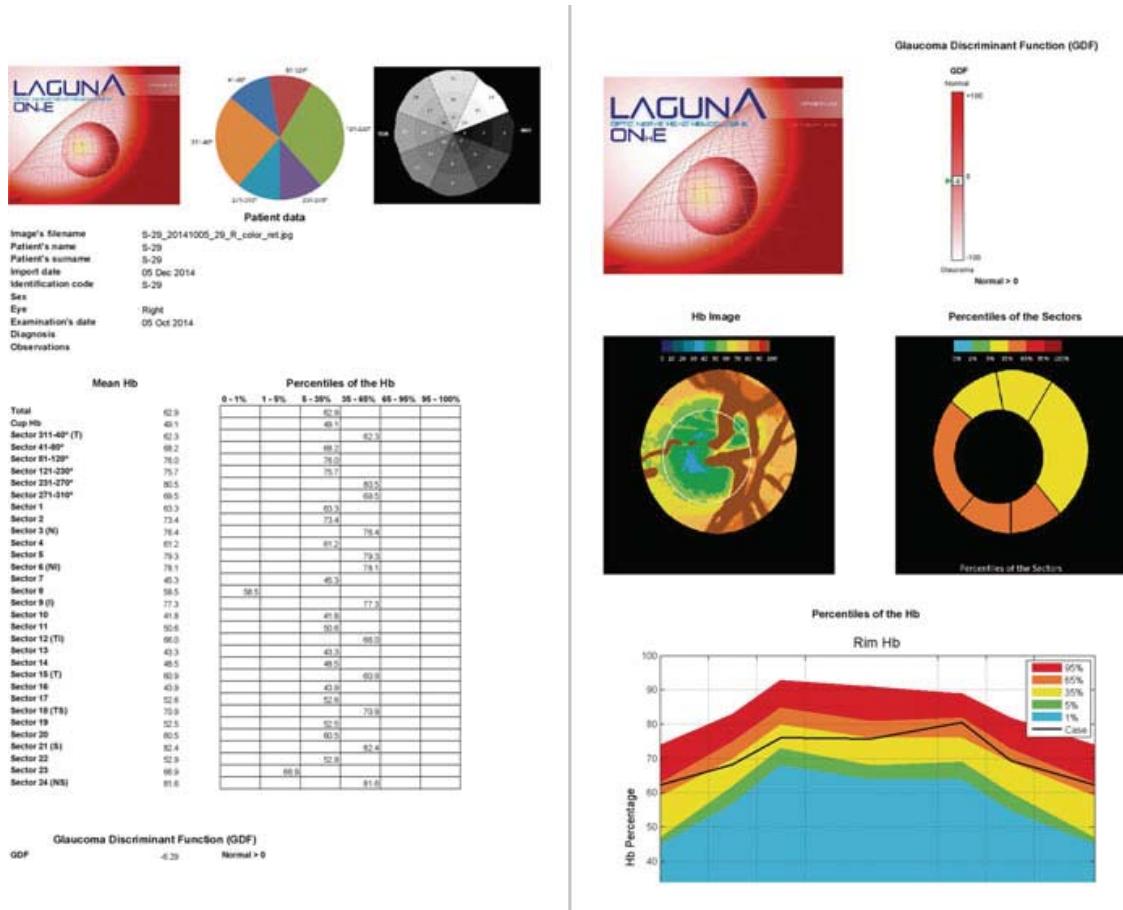


Fig. 10.17 Excel sheets showing results

10.9 Follow-Up

From the database of images for each patient, the tests can be recovered for overall analysis, and progression of the GDF index can be estimated by linear regression analysis (Fig. 10.18).

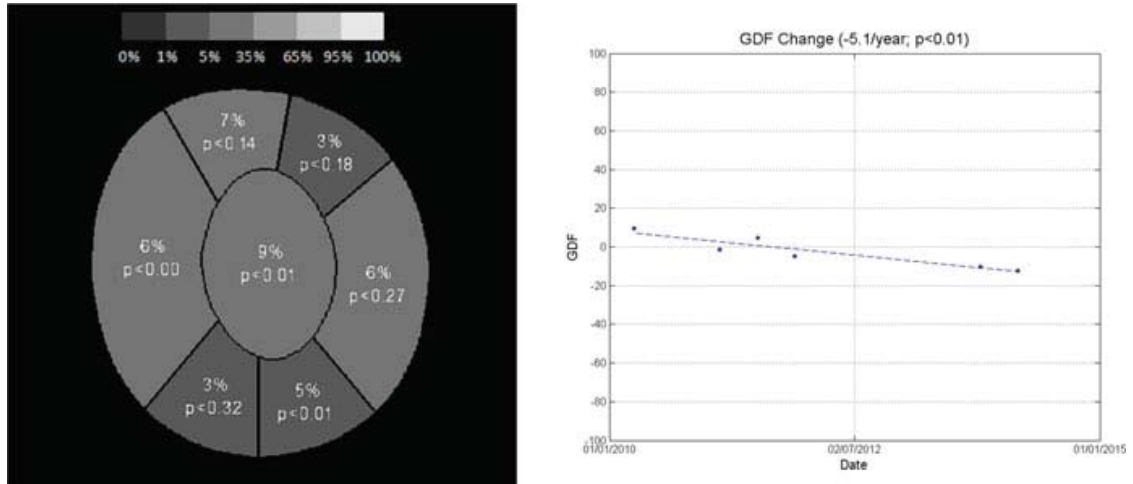


Fig. 10.18 Graphic representation of change in the amount of hemoglobin (*left*) and progression of GDF values (*right*)

Further Reading

1. Gonzalez de la Rosa M, Gonzalez-Hernandez M, Sigut J et al (2013) Measuring hemoglobin levels in the optic nerve head: comparisons with other structural and functional parameters of glaucoma. *Invest Ophthalmol Vis Sci* 54(1):482–489
2. Denniss J (2013) Estimation of hemoglobin levels in the optic nerve head for glaucoma management. *Invest Ophthalmol Vis Sci* 54(2):1515
3. Gonzalez de la Rosa M, Gonzalez-Hernandez M, Sigut J et al (2013) Author response: estimation of hemoglobin levels in the optic nerve head for glaucoma management. *Invest Ophthalmol Vis Sci* 54(3):2011–2012
4. Bambo MP, Garcia-Martin E, Perez-Olivan S et al (2013) Diagnostic ability of a new method for measuring haemoglobin levels in the optic nerve head in multiple sclerosis patients. *Br J Ophthalmol* 97(12):1543–1548
5. Bambo M, Garcia-Martin E, Perez-Olivan S et al (2014) Detecting optic atrophy in multiple sclerosis patients using new colorimetric analysis software: from idea to application. *Semin Ophthalmol*:1–4. doi:[10.3109/08820538.2014.962171](https://doi.org/10.3109/08820538.2014.962171)
6. Mendez-Hernandez C, Garcia-Feijoo J, Arribas-Pardo P et al (2014) Reproducibility of optic nerve head hemoglobin measures. *J Glaucoma*. 27 Oct 2014 [Epub ahead of print]. PMID: 25350818
7. Bambo MP, Garcia-Martin E, Satue M et al (2014) Measuring hemoglobin levels in the optic disc of Parkinson's disease patients using new colorimetric analysis software. *Parkinsons Dis* 2014:946540
8. Pena-Betancor C, Gonzalez-Hernandez M, Fumero-Batista F et al (2015) Estimation of the relative amount of hemoglobin in the cup and neuroretinal rim using stereoscopic color fundus images. *Invest Ophthalmol Vis Sci* 56(3):1562–1568
9. Bambo MP, Garcia-Martin E, Gutierrez-Ruiz F et al (2015) Analysis of optic disk color changes in Alzheimer's disease: a potential new biomarker. *Clin Neurol Neurosurg* 132:68–73